Chemistry and Materials Research
ISSN 2224- 3224 (Print) ISSN 2225- 0956 (Online)
Vol.6 No.12, 2014

Effect of the Different Preparation Methods on the Characterization and the Catalytic activity of the Nano-Structured Cryptomelane Materials

S. Said[1] M. Riad[1*] M. Helmy[1] S. Mikhail[1] L. Khalil[1,2]
1. Egyptian Petroleum Research Institute
2. Faculty of Science Ain Shams University
[*]E-mail of corresponding author: maryriad2006@yahoo.com

Abstract
Manganese-based octahedral molecular sieves of the type K-OMS-2 (cryptomelane structure) were prepared either by synproportionation of $KMnO_4$ and Mn^{2+}sulfate salts, in acidic aqueous suspension (reflux method) and or by the reduction of Mn^{+7} using benzyl alcohol and CTAB (as template) in neutral medium. The prepared K-OMS-2 materials were characterized using several techniques: X-ray diffraction, Fourier transformer-Infrared & Raman spectroscopy, Transmission electron microscopy, differential & gravimetric thermal analysis, H_2-temperature programmed reduction and N_2 adsorption-desorption measurements. The results revealed that, the two prepared samples are mainly nano-structured cryptomelane materials (crystallite diameter 9- 32.5 nm.). The obtained K-OMS-2 material on using the sulfate anion (reflux method) has more available lattice oxygen as compared to that prepared by the other method. On using CTAB the obtained cryptomelane material exhibits a high thermal stability. The catalytic activity of the prepared K-OMS-2 cryptomelane samples were studied towards the oxidation reaction of cyclohexane at reaction temperature: 300-400^oC. The catalytic activity for K-OMS-2 "neutral" is higher (the conversion increases with the increase in reaction temperature from 27 to 95% successively) with respect to K-OMS-2 "reflux" (the conversion increases from 30 to 79% successively).
Keywords: Cryptomelane, acidic, neutral, lattice oxygen, thermal stability.

Introduction

Cryptomelane (K-OMS-2), an octahedral molecular sieve, is an allotropic form of manganese oxide having a well-defined 2×2 tunnel structure. K-OMS-2 is constructed from edge-shared double chains MnO_6 octahedra units that are corner connected to form an open tunnel of 4.6 by 4.6A^o size. Potassium ions are situated inside the tunnels to provide charge balance and to stabilize the structure (chemical composition = $KMn_8O_{16}.nH_2O$). The diameters of the tunnel cross sections are in the range of that typical for zeolite pores. Due to its porous structure, hydrophobic nature, easy release of lattice oxygen, acidic sites and mixed valence of manganese species, cryptomelane has been extensively explored for potential applications such as molecular sieves, a low cost-efficient, and environmentally friendly catalysts. It has gained a good reputation in redox catalysis alternative to the conventional catalysts such as supported noble metals (Suib, 2008). Several different morphologies have been synthesized ranging from micrometer long fibers to nano-rod sand paper like materials (Peluso et al., 2008), Different methods have been reported for preparing K-OMS-2 depending on refluxing a mixture of potassium permanganate and manganese sulfate in an acidic medium (Villegas et al., 2005, Portehault et al., 2009, Zhu et al., 2012, Sun et al., 2013, Dharmarathna et al., 2014) . Sithambaramaet et al., (2010) prepared K-OMS-2 by the reflux method and investigated their activity for hydrogen generation via the water-gas shift reaction.

Sun et al., (2011) prepared K-OMS-2 materials (by a solid-state and reflux methods) to study the catalytic oxidation of toluene. The results established that K-OMS-2 prepared by the refluxing method exhibited higher catalytic activity than that by the solid-state reaction method. It was apparent that the high catalytic activity of the prepared K-OMS-2 by the refluxing method is attributed to the more available lattice oxygen and the higher oxygen mobility.

Tian et al., (2011) prepared porous manganese oxide K-OMS-2 nano-materials by a simple low-temperature in neutral medium method.

Deng et al., (2014) prepared (K-OMS-2) of rod-like, fibrous-like, and nest-like morphologies by solid-state reaction, reflux and hydrothermal methods, respectively. The materials were characterized and tested for liquid-phase oxidation of p-chlorotoluene to p-chlorobenzaldehyde. Over nest-like K-OMS-2, p-chlorotoluene conversion was significantly higher than that of the others.

In the current work, low cost K-OMS-2 materials were prepared via reflux (acidic), and reduction (neutral medium) methods. The diversity of the properties of the obtained materials depending on the preparation medium that including morphologies, crystallite size and lattice oxygen were investigated. In addition, the catalytic activity of the prepared cryptomelane samples was studied towards the oxidation reaction of cyclohexane under the experimental variable conditions.

2. Experimental

2.1. Preparation of K-OMS-2

2.1.1. Reflux Method "acidic medium"

K-OMS-2 was prepared through the oxidation of manganese sulfate by potassium permanganate in an acidic medium under reflux according to the procedure described by DeGuzman et al., (1994) A solution of 0.4M potassium permanganate (13.3 g) was dissolved in 225 ml of distilled water at room temperature, 6.7 ml of nitric acid (65 wt.%) was also added to adjust pH value "3.5". This solution was added to a second one consisting of 19.8g $MnSO_4.H_2O$ (1.75 M) dissolved in 67.5 ml of distilled water (under continuous stirring). The resulting solution was transferred to a 500 ml round-bottomed flask fitted with a reflux condenser, stirred vigorously and refluxed at a temperature of 100 ^oC for 24 h. The formed dark brown precipitate is filtered, washed until pH= 7 and then dried at 120 ^oC overnight. The prepared sample is denoted as K-OMS-2RS.

2.1.2. Reduction Method "Neutral Medium"

K-OMS-2 was prepared in neutral medium at room temperature, as described by Tian et al., (2014). 0.364 g (1 mmol) cetyltrimethylammonium bromide (CTAB) and 1.622 g (15 mmol) benzyl alcohol (reducing agent) were dissolved in 100 ml of distilled water under stirring, and then a solution of 1.580 g, $KMnO_4$ (1.0 M) dissolved in 100 ml distilled water, was added to this mixture. The reaction proceeded with the appearance of a brown precipitate within a few minutes. After a reaction time of 16 hours, the precipitate was filtrated, washed several times with distilled water and alcohol, and dried overnight at 60 ^oC. The product was then calcined at 550 ^oC for 6 hours to get rid of the surfactant. The prepared sample is denoted as K-OMS-2N.

2.2. Structural Phase Changes

Different techniques were applied to investigate the physico-chemical characteristics of the prepared K-OMS-2 materials.

2.2.1. X-ray Powder Diffraction Analysis (XRD)

The structure and phase purity of the prepared materials were analyzed via X-ray diffraction (XRD). The experiments were carried out using a Shimadzu XD-1 diffractometer using Cu K_α radiation (λ = 0.1542 nm) at a beam voltage of 40 kV and 40 mA beam current. The intensity data were collected at 25^oC in a 2θ range of 10-70^{o}with a scan rate of 0.7$^\circ s^{-1}$. The Joint Committee on Powder Diffraction Society (JCPDS) database was used to index the peaks of XRD.

Average Crystallite Size was calculated from X-ray line broadening using Sherrer's equation at 2θ = 37.8^o characterized the prepared materials.

2.2.2. Fourier Transformer Infra-Red Spectroscopy

Fourier transform infrared (FTIR) spectroscopy experiments were performed on a spectrometer Perkin-Elmer – Spectrum-1 in the range of 4000–400 cm^{-1} at a resolution of 4 cm^{-1}. The samples were grounded to fine powder and dispersed in KBr to compress into pellets before measurement.

2.2.3. Raman spectroscopy

Raman spectra were recorded at room temperature in the range of 100–1000 cm^{-1} with a HR – UV 800 Confocal Scanning Spectrometer (Horiba JobinYvon), equipped with a Peltier –cooled charge coupled device (1152x 298 pixels), the spectral resolution was 0.5cm^{-1}. The Raman scattering was excited using a 632.81 nm excitation wavelength supplied by an internal He–Ne laser through an Olympus high-stability BXFM confocal Microscope.

2.2.4. Thermal Analysis

Differential thermal (DTA) and thermogravimetric (TG) analyses were performed to study the structural changes of the prepared materials with thermal treatment. 10 mg of sample was heated up to 1100 ^OC, with a heating rate of 10^oC min^{-1} in airflow at a rate of 50 ml min^{-1} on SDTQ-600 (TA-USA) thermo balance instrument.

2.2.5. High resolution transmission electron microscopy (HRTEM)

The morphologies of the prepared materials were studied using high-resolution transmission electron microscopy. HRTEM images of the materials were obtained in JEOL JEM-2100F microscope operating at voltage of 200 kV. The samples were prepared by dispersing in ethanol and sonicated for 20 min. The suspension was then dropped on a carbon coated copper grid for TEM observations.

2.2.6. Temperature Programmed Reduction (TPR)

Temperature programmed reduction experiment were carried out to investigate the redox properties (the ease of reducibility of metal oxide) for the studied materials. The experiments were performed in automatic equipment (Chembet 3000, Quantachrome). Typically 100mg of calcined material was loaded into a quartz reactor and heated under inert atmosphere (20ml/min N_2) at 200^oC for 3 hours prior to running TPR experiments, and the cooled down to room temperature in N_2. Then the sample was submitted to a constant rate of heat treatment (10^oC/min up to 1000^oC) in a gas flow (mixture H_2/N_2, 5/95 vol%, reducing gas) 80ml/min. A thermal conductivity detector (TCD) was employed to mintor the amount of hydrogen consumption.

2.2.7. N_2 Adsorption- Desorption Isotherms

Surface area and pore structure characteristics of the prepared cryptomelane samples as the specific surface area

(S_{BET}), total pore volume (V_p) and average pore diameter (dp A^o) were measured from N_2 adsorption-desorption isotherms at liquid nitrogen temperature (-198^{o}C) using Quanta chrome Nova 3200 S automates gas sorption apparatus. Prior to such measurements, all samples were perfectly degassed at 200^{o}C for 12hr. and under vacuum pressure 1.3x 10^3 Pa.

2.3. Catalytic activity

The gas phase oxidation of cyclohexane was carried out in a fixed bed vertical downward flow glass reactor (internal diameter 6 mm), operated under atmospheric pressure. About 2ml of the pretreated catalyst was placed at the hot zone of the reactor supported on either side with a thin layer of quartz wool and ceramic beads. The reaction temperature was monitored by a thermocouple placed in the middle of the catalyst bed. The catalyst was activated at 250 ◦C for 2 h before reaction in a controlled stream of air as a carrier gas with flow rate of 50 ml min^{-1}. The cyclohexane reactant was fed into the reactor with the required flow rate (3ml/hr.) using a syringe infusion pump. The collected products in the receiver flask, were analyzed in a gas chromatograph (Shimadzu 17A) equipped with a DB-5 capillary column (30 m × 0.25 mm × 0.25 mm) and a flame ionization detector.

3. Results and Discussions

3.1. X-ray Diffraction Analysis (XRD)

A- Cryptomelane K-OMS-2RS prepared sample

X-ray diffraction pattern for K-OMS-2RS is depicted in Fig.(1-a). The pattern reveals the appearance of diffraction peaks at 2θ=12.8°, 18.5°, 28.9°, 37.5°, 42° and 50°, these peaks are consistent with those of the standard cryptomelane (K-OMS-2) material with tetragonal symmetry corresponding to KMn_8O_{16}, (JCPDS 29-1020), which emphasized that the resulting material is a pure mono-phasic cryptomelane structure.

The **average Crystallite Size** was calculated from X-ray line broadening using Sherrer's equation at 2θ = 37.5^o and it is found to be 26.6 nm.

B- Cryptomelane K-OMS-2N prepared samples

X-ray diffraction pattern (Fig.1-b&c) for K-OMS-2N represents broad low intense peaks assigned at 2θ=18.5°, 28.9° and 37.2^o which are characterized for the formation of cryptomelane material.

It was proposed that benzyl alcohol might be inserted between the molecules of CTAB surfactant **Durmus et al., (2010)**, and contributed in the formation of K-OMS-2 material that caps their characteristic lines. Accordingly, the interaction between the $(CH_3)_3–N^+$ hydrophill group of CTAB and the oxygen atoms of the formed OMS, cause the pseudo-disappearance of the most of OMS-2 characteristic lines.

Upon calcination, the XRD pattern reflects the appearance of sharp and high intense diffraction lines. The destruction of CTAB upon thermal treatment allows the diffraction lines characterized the cryptomelane material to appear at 2θ=12.8°, 18.5°, 28.9°, 37.5°, 42° and 50°. The cryptomelane phase constructed by CTAB shows an increase in diffraction line intensities compared to that prepared by the other method.

In fact, CTAB interacts with the reactant molecules and affects their packing and degree of ordering, with the different degrees of the preferred growth orientation along the c-axis as indicating from the high crystallinity of the resulting material. Thus, the produced material is a pure cryptomelane-type crystalline phase.

The crystallite size was found to be 38.74 nm. Due to the templating effect of CTAB, the primary manganese oxide crystallites is easy to agglomerate owing to its high surface energy which resulting in large crystallite size, in parallel with the sharpness of XRD lines.

3.2. Fourier Transformer Infrared

A- Cryptomelane K-OMS-2RS prepared sample

The FT-IR spectrum for the prepared material via reflux technique is depicted in Fig. (2-a). The spectrum detects several bands at 475, 528, 713, 1618 & 3419 cm^{-1} .These bands are ascribed to the vibrations of the MnO_6 octahedral framework present a clear signature of cryptomelane structure (Gac, 2007). The vibration band located at 475 cm^{-1}, can be attributed to the vibration of the manganese species (Mn^{3+}) in the octahedral sites. The bands detected at 523 and 713 cm^{-1} are assigned to the vibration due to the displacement of the oxygen anions relative to the manganese ions along the direction of the octahedral chains, and the stretching mode of MnO_6 octahedra along the double-chain, respectively. The band appeared at 1120 cm^{-1} is attributed to Mn–O–H structural vibrations (Julien etal., 2004).

Meanwhile, the broad band detected at ~3419 cm^{-1} is assigned to the stretching vibration of the water molecule and OH^- in the lattice of cryptomelane material, and that at 1618 cm^{-1} is assigned to the bending vibration of water molecules in the tunnels and hydrogen bounded OH-groups, which implies that the hydroxyl groups exist in the prepared material.

B- Cryptomelane K-OMS-2N prepared sample

FT-IR spectrum for the prepared K-OMS-2N material (Fig.2-b) displayed bands around 450, 510, 600, 710, 963, 1383 and 3365 cm^{-1} that are characteristic for cryptomelane material.

The band assigned at 1531cm^{-1} corresponds to the C= C stretching vibration in the aromatic benzene ring. The intense bands located at 2850 and 2914 cm^{-1} are assigned to the symmetric and asymmetric stretching modes of the $–CH_2$ group of the CTAB surfactant. The symmetric and asymmetric scissoring vibrations of $(CH_3)_3–N^+$ group of CTAB are assigned at 1510 cm^{-1}. The single band located at 930 cm^{-1} may be assigned to the $(C–N^+)$ stretching mode of CTAB (Durmus et al., 2010).

The absence of the vibration band characteristic to benzyl alcohol at 3620 cm^{-1} established that there is an interaction between the oxygen atoms of the $Ph-CH_2-O-H$ and the $–CH_2$ groups belonging to the CTAB surfactant(C–H· · · O), which then combines with the hydrophilic head of CTAB and contributes in the formation of K-OMS-2,in agreement with XRD results.

After thermal treatment, the vibration bands corresponding to the surfactant molecules were disappeared (Fig.2-c), indicating that all organic groups were destructed via calcination process. On the other hand, the IR spectrum clarified the vibrational bands characterize to the cryptomelane material (535, 600, 712, 1627 & 3466 cm^{-1}).

More pronounced increase of % Transmittance for the band appeared at ~ 3400 cm^{-1} which is related to the increase in the amount of hydroxyl groups or tunnel water species for the prepared materials, it increases from sulfate> neutral.

3.3. Raman spectroscopy

A- Cryptomelane K-OMS-2RS prepared sample

Raman spectroscopy for the prepared material K-OMS-2RS (Fig.2-a) reveals the appearance of Raman signals centered at 142, 250, 360, 544 and 607 cm^{-1}**.** Peak detected at 544 cm^{-1} is assigned to the vibration that due to the displacement of the oxygen anion (relative to the manganese ion) along the direction of the octahedral chains, whereas the vibration frequency at 607 cm^{-1} is assigned to Mn-O stretching mode in tetrahedral sites environment, as confirmed by FT-IR. Meanwhile, the signal at 142, 250& 360 cm^{-1} are due to the Mn–O–Mn bending vibration in the MnO_2 octahedral lattice (Kim, Stair, 2004). From Mn–O stretching range, the two sharp, high-frequency Raman bands at 544 &607 $cm^{-1}$are indicative of a well-developed tetragonal structure with an interstitial space consisting of (2×2) tunnels of cryptomelane material (Julienet al., 2004, Gao et al., 2008).

B- Cryptomelane K-OMS-2N prepared sample

Raman spectra for the prepared K-OMS-2N material and the calcined one are represented in Fig (2-b&c). The spectrum for the prepared material reveals the appearance of two bands at 571 &636 cm^{-1} which are assigned to the Mn–O stretching of MnO_6 octahedra that confirm the formation of cryptomelane material. The disappearance of the low frequency bands characterize cryptomelane material may be result from the inter-chelation of CTAB within the formed material, in agreement with XRD results.

Upon calcination Raman spectrum reveals the appearance of low and high frequency signals at, 149, 345, 470, 578 & 627 cm^{-1} with a low intensity. These signals are characteristics for the formation of cryptomelane material.

3.4. Differential and Gravimetric Thermal Analysis (DTA& TGA)

A- Cryptomelane K-OMS-2RS prepared sample

Differential and Gravimetric thermal analysis profiles for the sample K-OMS-2RS is represented in Fig. (3-a). DTA profile displayed one exothermic peak at 190^oC, and three endothermic peaks located at 569, 849 and 967 ^oC “centered at 202, 555, 855 & 969 ^oC, as confirmed from the dDTA profile". The exothermic peak may be corresponded to the formation of crystalline phase, i.e. the over oxidation of sulfate anion which may still present on the surface of the prepared material. Meanwhile, the endothermic peak at 569 ^oC is an indication for the desorption of water inside the (2x2) tunnels, as stated by Suib (2008). The second and third endothermic peaks are corresponding to the phase transformation of MnO_2 into Mn_2O_3 and Mn_2O_3 into Mn_3O_4, respectively.

The previous thermal effects are accompanied by steps of weight losses. TG profile (Fig.3-a) demonstrates that 5% weight losses at the temperature range 50-250, could be due to the depletion of the physically and chemisorbed water molecules either on the surface and or on the channel structure (Hndel etal., 2013). With the increase in the temperature to 750°C the weight loss increases to 6.6% which is due to the release of the water molecules inside the tunnels, besides the desorption of the structural oxygen that closed to the surface(related with the formation of lattice vacancies without decomposition of the material). The weight losses “~ 1 at the temperature range 750◦C - 950 ◦C and 2.6% at the temperature up to 950 ◦C” imply the transformation of cryptomelane to bixbyite (Mn_2O_3) and then to Hausmannite (Mn_3O_4) species (Cheng et al., 2011), with total weight loss 15.44%. Thus, there are plenty of lattice oxygen species in the produced OMS-2RS

material, which become more easy to mobile upon thermal treatment (in agreement with the Raman spectroscopic results).

B- Cryptomelane K-OMS-2N prepared sample

Differential thermal analysis for K-OMS-2N material is displayed in Fig. (3-b) and reflects the appearance of three exothermic and one endothermic peaks. The three exothermic peaks are appeared at 186, 212 &490^{o}C "centered at 185, 225& 485^{o}C, as confirmed from the d (DTA) profile" are related to the release of weakly adsorbed water molecules and to the removal of the organic entities of CTAB surfactant. The thermal degradation of the pure CTAB is separately recorded, showing endothermic peaks started from 200 to 500^{o}C. In agreement with, Tian et al., (2014) who stated that the degradation of CTAB is completely occurred at 500^{o}C. The endothermic peak detected at 880^{o}C is related to the decomposition of cryptomelane to Mn_2O_3 species.

The absence of the endothermic peak at 600 ^{o}C characterize the labiality of lattice oxygen demonstrates a progress in their thermal stability given by CTAB which act as an occupator reinforce toughen the oxygen-Mn linkage, and reflect the maintenance of the attached water or the hydroxyl group in the cryptomelane tunnel structure (in agreement with FT-IR results).

TG profile for K-OMS-2N material (Fig. 3-b) shows weight loss steps: at temperature range 50- 280^{o}C (47.89%) that related to the decomposition of CTAB moieties. The step in the temperature range 480-800^{o}C is due to the desorption of structural oxygen close to the surface, this step is accompanied by slight weight gain 0.75% which implies the stability of the formed material and the restriction of lattice oxygen for desorption. The weight loss at 840-920 ^{o}C (1.93%) is due to the decomposition of cryptomelane to Mn_2O_3 species, in parallel with the results of differential thermal behavior.

3.5. Transmission Electron Microscopy (TEM)

A- Cryptomelane K-OMS-2RS prepared sample

TEM image for nano sized -particles K-OMS-2RS material shows agglomerated or clusters of disorderly stacked rod-like crystals with an average diameter 9 nm (Fig.4). In addition, It is evident that the degree of dispersion for the prepared cryptomelane particles is high, in agreement with Walanda et al., study (2005).

B- Cryptomelane K-OMS-2N prepared sample

TEM image for uncalcined K-OMS-2N, Fig.5-a) detects large particles of CTAB around the formed cryptomelane rods which seemed to grow with a short length, (in agreement with XRD and Raman spectroscopy results).

For the calcined material at 200^{o}C, the image (Fig.5-b) shows that the cryptomelane rod structure started to be lengthening once the CTAB molecules contracted in their size, upon the gradual decomposition up to 200^{o}C.

After calcination, at 500^{o}C the TEM image (Fig.5-c) shows plates like structures of larger and longer particles (32.5 nm.). As well known, the benzyl alcohol contributes in the reaction solubilized in the interfacial region of the formed cryptomelane aggregates, which promotes the rod micelles to be larger and longer.

The discrepancy in the crystallite diameter data (26.6 - 38.74 nm) confirmed by the x-ray diffraction analysis with that by TEM (9- 32.5 nm.) is due to the agglomeration among the primary particles.

3.6. H_2-Temperature Programmed Reduction

A- Cryptomelane K-OMS-2RS prepared sample

H_2-TPR profile for OMS-2RS (Fig. 6-a) detects four reduction peaks, two strong peaks at 383, 403^{o}C and the other are broad weak at 450, 650^{o}C, according to the postulated studies these peaks are related to the successive reduction steps as follow:

- $MnO_2 \rightarrow Mn_2O_3$
- $Mn_2O_3 \rightarrow Mn_3O_4$
- $Mn_3O_4 \rightarrow MnO$
- $MnO \rightarrow Mn^0$

As well known, the Mn-O bonds of K-OMS-2 are relatively weaker and the Mn species in OMS-2 can be reduced more easily at reduction temperature below 500^{o}C.

Besides, due to the bigger negative reduction potential of MnO, no reduction band assignable to the $MnO \rightarrow Mn^0$ process was observed even up to 750 ◦C. Therefore, the weak reduction peak observed at 650^{o}C may be related to the reduction of K_2SO_4 which may be still inter-chelated in the cryptomelane structure. Therefore, it is reasonably deduced that MnO was the final state of cryptomelane -MnO_2 reduction. The hydrogen consumption was 5.4.

B- Cryptomelane K-OMS-2N prepared sample

H_2-TPR for the material prepared via neutral technique (Fig.6-b) detected two reduction peaks at 372 &419^{o}C,

these are overlapped peaks corresponding to two-steps reduction process. Assuming that MnO is the final state in the reduction of OMS-2, this reduction peaks indicates that the MnO_2 was probably reduced to Mn_2O_3 then Mn_2O_3/ Mn_3O_4 to MnO, with hydrogen consumed 2.4 which is lower than that for K-OMS-2RS and implies the reducibility and reactivity of Mn-O bond is lower, in agreement with the previous results.

3.7. Nitrogen adsorption - desorption Isotherms and Porosity Analysis

The nitrogen adsorption - desorption isotherms of K-OMS-2RS and K-OMS-2N are shown in Figs. (7-a). The texture properties: surface area (S_{BET}), total pore volume (V_p) and average pore diameter**,** were complied in Table (1).

The pore size distribution for the samples have obtained from the desorption branch following the Barrette Joynere Halenda (BJH) procedure illustrated in the form of dV/dD vs. average pore diameter (D, nm) in Fig. (7- b).

The nitrogen adsorption–desorption isotherms (Fig. 7- a) for the two prepared samples show that the adsorption isotherms are related to type II according to Brunauer et al., classification (Brunauer et al., 1940) and are characteristic for cryptomelane materials in accordance with Malinger et al. (2006). The isotherms of the samples exhibits H3 type hysteresis loop according to IUPAC classification (Gregg and Sing, 1982). The type indicates the presence of the aggregation of plate-like nano-particles giving rise to slit-shaped pores, due to the inter-particle voids of the aggregated K-OMS-2 nano-rods, in agreement with the TEM data.

A - Cryptomelane K-OMS-2RS prepared sample

Data in Table (1) represents that K-OMS-2RS has high surface area 96.0 m^2/g, which reflect the predominate of narrow pores. According to TEM image, the agglomeration of the nano-fibers bunches showing meso-pores between the fibers which responsible for the high surface area. In spite, the high surface area value, the average pore diameter is shown to be of a high value 12.0 nm. This reflects the diffusion of the strong acidic sulfate species (large polar species) towards the narrow meso-pores, which may cause the opening up of some narrow regions to furnish a measurable area and expanded the pores. Upon removing the sulphate species, it leaves behinds pores with relatively large diameter.

Pore size distribution curve for K-OMS-2RS (Fig, 7-b) behaves a bi-modal contribution, the first one with a mean pore diameter ranging between (1.7- 4.3 nm.) and centered at ~ 3 nm with abundant 0.002, and the second broad one (4.3- 29.23 nm.) centered at ~ 12.0 nm with more abundant 0.0028 which demonstrates the presence of heterogeneous meso-pores structure.

B- Cryptomelane K-OMS-2N prepared sample

The surface area for K-OMS-2N stridently decreased, it decreases to 14m^2/g compared to K-OMS-2RS. This decrement may be resulting from the aggregation of the primary manganese oxide crystallites via temlpating effect of CTAB. The large crystallites cause tightening and thinning of the meso- pores and a decrease in the extent of surface area and total pore volume (0.04 cc/g), in consistent with the large crystallite size and TEM images. The average pore diameter, was 2.0 nm, this implies the generation of narrow meso-pores in the spaces between the formed large crystallites.

The pore size distribution for K-OMS-2N (Fig.7-b) exhibits meso-pores with two main different most probable diameters at 2 and 5 nm. This pores show a relatively narrow pore size distribution indicating a uniform mesopore diameter with abundant 0.0005, and 0.002 respectively. The nature of interaction between templates and manganese reactant controls the folding of templating agent, which forms the ordered narrow meso-phase during preparation.

3.2. Catalytic Activity

The gas phase oxidation reaction of cyclohexane was taken as a model reaction to investigate the catalytic activity of the prepared nano-structured K-OMS-2RS (9 nm.) & K-OMS-2N (32.5 nm) cryptomelane samples. The catalytic oxidation of cyclohexane is performed in a flow type system operating under atmospheric pressure and at the reaction temperature varying between 300- 400^oC, cyclohexane flow rate 3ml/hr, liquid hourly space velocity 1.5h^{-1} and with air flow rate of 50 ml/min. The results are graphically illustrated in Figs. (8-11).

Figure (8-a) clarifies the increase in the catalytic activity of the two prepared K-OMS-2 cryptomelane samples, with the increase in the reaction temperature, in agreement with the results of our previous work which demonstrated the dehydrogenation of cyclohexane using molybdenum supported mixed oxide catalysts at reaction temperature ranged from 250-550^oC (Riad and Mikhail, 2008) .

K-OMS-2N cryptomelane sample shows a sharp increase in its activity as the reaction temperature increases in the range from 300 to 400^oC (the conversion increases from 27 to 95% successively). While K-OMS-2RS sample shows lower activity with respect to the other sample (Histogram in Fig. 8-b), whereas it increases as the reaction temperature range from 300- 400 (the conversion increases from 30 to 79%

successively).

The converted products are mainly composed of oxygenated compounds, dehydrogenated compounds, alkylated aromatic compounds "liquid product" and gasses that include hydrocarbon gasses (C_1-C_4) and CO_2.

The converted products by increasing the reaction temperature over the prepared samples follow almost the same trend described above, i.e. the liquid and gasses products show a gradual increase with the increase in reaction temperature (Fig. 8-a).

From the relation between the reaction temperature and the distribution of the converted liquid products for K-OMS-2N sample, (Fig. 9), it can be observed that cyclohexene increases with the increase in the reaction temperature up to 375^{o}C and then decreases with further increase in reaction temperature to 400^{o}C which goes parallel with the increase in the formation of benzene and the alkylated aromatic compounds. The methanol and cyclohexanol show a gradual increase with the increase in reaction temperature up to 375^{o}C, meanwhile, the cyclohexanone product is found to increase gradually with the continuous increase in the reaction temperature.

For K-OMS-2RS sample, the relation between the reaction temperature and the distribution of the liquid converted product in Figure (9), reveals that the cyclohexene product increases with the increase in reaction temperature up to 350^{o}C. After that, it is sharply decreases (from 35% to 20% at reaction temperature up 400^{o}C) which is in parallel with the sharp increase in the alkylated aromatics products upon increasing the reaction temperature (from 12% at 350^{o}C to 29% at 400^{o}C).

The production of cyclohexanol and cyclohexanone has the same behavior with respect to K-OMS-2N sample.

In other words, the cyclohexanone product gradually increases with the increase in reaction temperature and the cyclohexanol shows a maximum at reaction temperature 375^{o}C.

Concurrently, from the relation between the reaction temperatures and the selectivity of the K-OMS-2 cryptomelane samples (Fig. 10) towards the formation of KA-oil (the catalytic oxidation of cyclohexane to cyclohexanone "K" and cyclohexanol "A" known as K-A oil). it is obvious that the formation of K-A oil gradually increases with the increase in reaction temperature up to 375^{o}C for both samples, and K-OMS-2N sample has highest catalytic activity (28%) with respect to K-OMS-2RS sample (19.5%). In agreement with the results obtained by Zhou et al., (2014) who investigated the cyclohexane oxidation using molecular oxygen as oxidant on Gold nanoparticles (Au@TiO2/MCM-41) and achieving a 9.87% conversion of cyclohexane, with selectivity 33.9 and 34.2% towards the formation of K and A respectively.

On the other hand for both samples, there is a little CO_2 produced at reaction temperature lowered than 350^{o}C , with increasing the reaction temperature, the CO_2 yield rises sharply to ~ 30% at 350^{o}C and then to 50% of the total produced gaseous products.

From the relation between the reaction temperature and the selectivity of the prepared cryptomelane samples towards the converted products, it can be observed that the selectivity towards the formation of the de-hydrogenated products (mainly cyclohexene for K-OMS-2RS) decreases with the increase in reaction temperature, which goes parallel with the gradual increase in the selectivity towards alkylated aromatic products (Fig. 11). Meanwhile the selectivity towards the oxygenated products increases with the increase in reaction temperature (Histogram in Fig. 11).

The variation in the catalytic activity of the prepared samples towards the cyclohexane conversion may be owing to the following:

The prepared OMS-2RS has:

- *a small crystallite size, high exposed surface area, high costituential water, high polarity and high adsorbed and dissociated molecular oxygen.*
- *high lattice oxygen close to the surface which increase the formation of lattice vacancies, increases unbalanced charges and lattice distortion occur on its surface, implies an increase of the electron density around Mn atoms, which result in an easy desorption of cyclohexene from the catalyst surface, and*
- *bi-modal pore size with diameter at 3, 12 nm. which may restricted, hindered and delaying the obtained products leads to an observed decrease in the total conversion,…… and*

The prepared OMS-2N has:

- a large crystallite size, narrow pore size distribution with diameter, 2 & 5 nm, the reaction is mostly occurred on the surface, and
- low costituential water, low polarity decrease of the electron density around Mn atoms, which result in constrict of the formed cyclohexene to complete the dehydrogenation route to benzene and alkylated benzene and consequently an increase in the total conversion is obtained.

4. Reaction Mechanism

According to the constituent of the converted products either liquid or gaseous that resulted from cyclohexane

conversion over the studied cryptomelane samples it may be assumed that the catalytic conversion of cyclohexane was accompanied by various reactions like dehydrogenation, oxidation, alkylation, disproportionation and cracking reactions.

The dehydrogenation reaction is preceded by the Mars–van Krevelen reaction mechanism (Gracia et al., 2009), in which adsorbed cyclohexane reacts with lattice oxygen and the reduced metal oxide reacts with adsorbed, dissociated oxygen. Oxidative dehydrogenation mechanism is discussed as followed: gaseous oxygen participates in the reaction only after adsorption in other parts of the catalyst and then migrates through the lattice to the active sites by the reoxidation between Mn^{3+} and Mn^{4+}. Mn^{4+}-O is responsible for providing the center of oxidation for the adsorbed alkyl species, which contributes to a high conversion of cyclohexane and a high selectivity to COx, whereas Mn^{3+} -O is responsible for activating cyclohexane and adsorbing oxygen, which attributes a high selectivity to cyclohexene.

Besides, the facility of oxygen dissociation in metal-based catalyst by transferring an electron to metal center, which is then back-donated to the antibonding orbital of the oxygen molecule.

The adsorbed cyclohexene is still subjected to two postulated ways depending on the available lattice oxygen:

- The intermediate formation of an alcohol by the addition of atomic oxygen to the cyclohexene. The alcohol may be either directly oxidized to an aldehyde or ketone, or dehydrated to cyclohexene, which, in turn, is oxidized at the double bond into an aldehyde or a ketone.

- the facile removal of subsequent hydrogen from cyclohexene to give adsorbed cyclohexadiene then adsorbed benzene which may be desorbed or converted to alkylated benzene: toluene, xylene, and tri-methyl benzene.

Conclusion

Nano-structured cryptomelane material (octahedral molecular sieve manganese oxide) with average crystallite size (9- 32nm.) are prepared either via reflux of Mn^{+7}andMn^{+2}(sulphate anion) in acidic medium, and or reducing of Mn^{+7} with benzyl in neutral medium in presence of CTAB as template.

From the study of the structural characterization and the morphology of the prepared cryptomelane samples, it may be concluded that:

- The prepared samples are mainly pure cryptomelane one.
- The sample prepared via reflux technique (K-OMS-2RS) has a lowest crystallite size (26.6 nm), meanwhile the crystallite size for the prepared sample via reduction technique (K-OMS-2N) is 38.6 nm (XRD analysis).
- The prepared cryptomelane samples have tetragonal structure with an interstitial space consisting of (2×2) tunnels. OMS-2N has the lowest tunnel water and most distorted tunnel structure "FT-IR and Raman spectroscopy".
- K-OMS-2N sample is the most stable compared to K-OMS-2RS one "TGA"
- The two prepared samples are formed in the nano-scale range 8 & 32.5 nm for K-OMS-2RSand K-OMS-2N, respectively "TEM".
- From the study of the catalytic activity of the prepared nano-sized cryptomelane K-OMS-2RS & K-OMS-2N samples toward the oxidation reaction of cyclohexane, it was found that:

- The two prepared samples exhibit high catalytic activity towards the oxidative- dehydrogenation of cyclohexane at the reaction temperature range (350-400^{o}C).
- The two prepared samples have high selectivity towards the formation of cyclohexene at lower reaction temperature 300^{o}C which decreases with the increase in reaction temperature which goes parallel with the gradual increase in the selectivity towards the alkylated aromatic products.

In addition, the prepared nano-structured K-OMS-2N cryptomelane catalyst offers an attractive solution for the production of K-A oil from the oxidative reaction of cyclohexane.

References

Brunauer,S., Deming, L. S., Deming, W. E., Teller, E. E. (1940). On a Theory of the van der Waals Adsorption of Gases, J. Am. Chem. Soc. 62, 1723.

Cheng, F.K., He, C., Shu, D., Chen, H., Zhang, Y. J., Tang, S.Q. (2011). Preparation of nanocrystalline VN by the melamine reduction of V_2O_5xerogel and its supercapacitive behavior, Mater. Chem. Phys., 131, 268–273.

Deng, Y., Zhang, T., Au , C., Yin, S. (2014). Oxidation of p-chlorotoluene to p-chlorobenzaldehyde over manganese-based octahedral molecular sieves of different morphologies, Catal. Commun., 43, 126–130.

DeGuzman, R., Shen,Y., Neth, E., Suib, S., O'Young, C., Levine, S., Newsam, J. (1994). Synthesis and Characterization of Octahedral Molecular Sieves (OMS-2) Having the Hollandite Structure, Chem. Mater., 6, 815–821.

Durmus, Z., Tomas, M,. Baykal, A., Kavas, H., Gürkaynak Altinçekiç, T., Toprak, M.S. (2010). The effect of neutralizing agent on the synthesis and characterization of Mn_3O_4nanoparticles, Russ. J. Inorg. Chem., 55,

1947–1952.
Dharmarathna, S., Kingòndu, C., Pahalagedara, L., Kuo, C., Zhang, Y., Suib, S. (2014). Ion Induced Promotion of Activity Enhancement of Mesoporous Manganese Oxides for Aerobic Oxidation Reactions, Appl. Catal. B: Envir., 147, 124– 131
Garces, L.J., Gomez,S., Durand, J.P., Suib, S.L. (2005). Particle Size Control of Cryptomelane Nanomaterials by Use of H_2O_2 in Acidic Conditions, Chem. Mater., 17, 1910–1918.
Gac,W. (2007). The influence of silver on the structural, redox and catalytic properties of the cryptomelane-type manganese oxides in the low-temperature CO oxidation reaction, Appl. Catal. B: Envir., 75, 107–117.
Gao,T., Glerup, M., Krumeich, F., Nesper, R., Fjellvg, H., Norby, P. (2008). Microstructures and Spectroscopic Properties of Cryptomelane-type Manganese Dioxide Nanofibers, J. Phys. Chem. C, 112, 13134–13140
Gracia J. M., Prinsloo F. F., Niemantsverdriet , J. W. (2009). Mars-van Krevelen-like Mechanism of CO Hydrogenation on an Iron Carbide Surface Catal Lett 133, 257–261
Gregg, S.J., Sing, K.S.W. (1982). Adsorption, Surface Area and Porosity, 2nd Edn, Academic Press Inc., London,.
Hndel ,M., Rennert ,T., Totsche, K. (2013). Synthesis of cryptomelane- and birnessite-type manganese oxides at ambient pressure and temperature, J. Collo. Inter. Sci., 405, 44–50 .
Julien, C.M., Massot, M., Poinsignon, C. (2004). Lattice vibrations of manganese oxides: Part I. Periodic structures, Spectrochim. Acta A, 60, 689–700.
Julien, C.M., Massot, M., Poinsignon, C. (2004). Synthesis characterization and biological study of diorganotin(IV) complexes of monomethyl phthalate, Spectrochim. Acta A, 60, 689- 694.
Kim, H.S., Stair, P. (2004). Bacterially Produced Manganese Oxide and Todorokite: UV Raman Spectroscopic Comparison, J. Phys. Chem. B, 108, 17019-17035 .
Malinger, K.A., Ding, Y., Sithambaram, S., Espinal, L., Gomez, S., Suib, S. L. (2006). Microwave frequency effects on synthesis of cryptomelane-type manganese oxide and catalytic activity of cryptomelane precursor, J. Catal. , 239 , 290- 297.
Peluso, M.A., Gambaro, L.A., Pronsato, E., Gazzoli,D., Thomas, H.J., Sambeth, J.E. (2008). Synthesis and catalytic activity of manganese dioxide (type OMS-2) for the abatement of oxygenated VOCs, Catal. Today, 133, 487–492.
Portehault, D., Cassaignon, S., Baudrinc, E., Jolivet ,J.P. (2009). Structural and morphological control of manganese oxide nanoparticlesupon soft aqueous precipitation through MnO_4^-/Mn^{2+} reaction, J. Mater. Chem., 19,
2407–2416.
Riad, M., Mikhail, S. (2008). Dehydrogenation of cyclohexane over molybdenum/mixed oxide catalysts, Catal. Comm., 9 , 1398.
Suib, S.L. (2008). Porous Manganese Oxide Octahedral Molecular Sieves and Octahedral Layered Materials, Acc. Chem. Res., 41, 479–487. [3] Villegas, J.C.,
Sun , M., Yu , L., Ye , F., Diao, G., Yu ,Q., Hao , Z., Zheng , Y., Yuan, L. (2013). Transition metal doped cryptomelane-type manganese oxide for low-temperature catalytic combustion of dimethyl ether, Chem. Eng. J., 220, 320–327.
Sithambarama, S., Wenc, W., Njagia, E., Shenb, X., Hansonc, J., Suiba, S. (2010). H_2 production through the water-gas shift reaction: An in situ time-resolved X-ray diffraction investigation of manganese OMS-2 catalyst, Catal. Today, 156, 2–7.
Sun, H., Chen, S., Wang, P., Quan, X. (2011). Catalytic oxidation of toluene over manganese oxide octahedral molecular sieves (OMS-2) synthesized by different methods, Chem. Eng. J., 178, 191– 196.
Tian, H., He, J. Zhang , X., Zhou ,L., Wang,D. (2011). Highly active manganese oxide catalysts for low-temperature oxidation of formaldehyde, Micropor. and Mesopor. Mater., 138, 118–122.
Walanda, D,. Lawrance, G., Donne, S. (2005). Hydrothermal MnO_2: synthesis, structure, morphology and discharge performance, J. Pow. Sour., 139, 325–41.
Zhou , J. Yang,X. Wang, Y. Chen, W. (2014). An efficient oxidation of cyclohexane over Au@TiO_2/MCM-41 catalyst prepared by photocatalytic reduction method using molecular oxygen as oxidant. Catal, Comm., 46, 228-236.
Zhu, M., Farrow ,C., Post, J., Livi , K., Billinge, S., Ginder-Vogel , M., Sparks, D. (2012). Structural study of biotic and abiotic poorly-crystalline manganese oxides using atomic pair distribution function analysis, Geoch. et Cosmochimica Acta, 81, 39–55.

Table1. The textural properties of the K-OMS-2N and K-OMS-2RS prepared samples.

Sample name	Crystallite size		S_{BET} (m^2/g)	$T.V_p$(cc/g)	D_p(nm)
	XRD	TEM			
K-OMS-2N	**38.7**	**32.5**	**14**	**0.04**	**2**
K-OMS-2RS	**26.6**	**9**	**96**	**0.3**	**12**

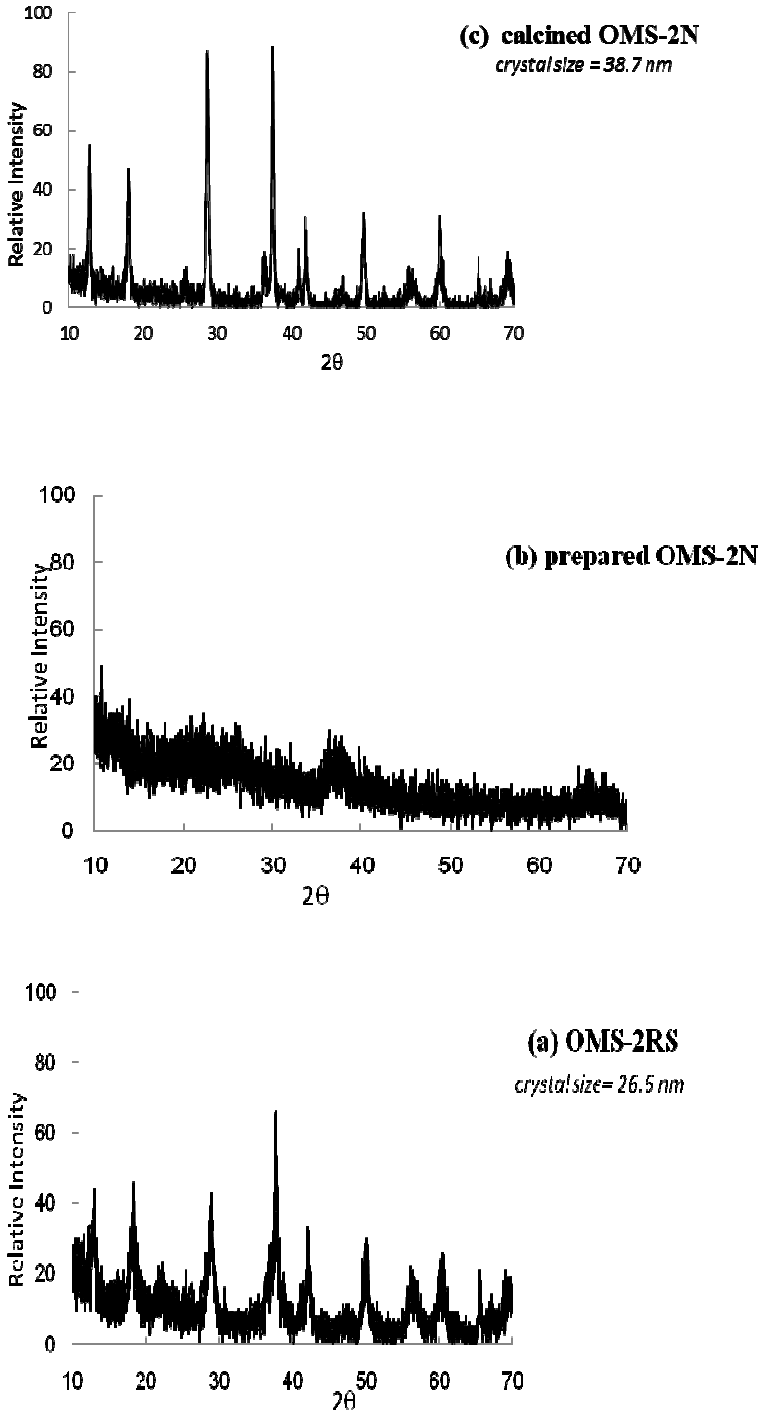

Fig.1. X-ray diffraction patterns of (a) K-OMS-2RS (b) prepared K-OMS-2N & (c) calcined K-OMS-2N samples.

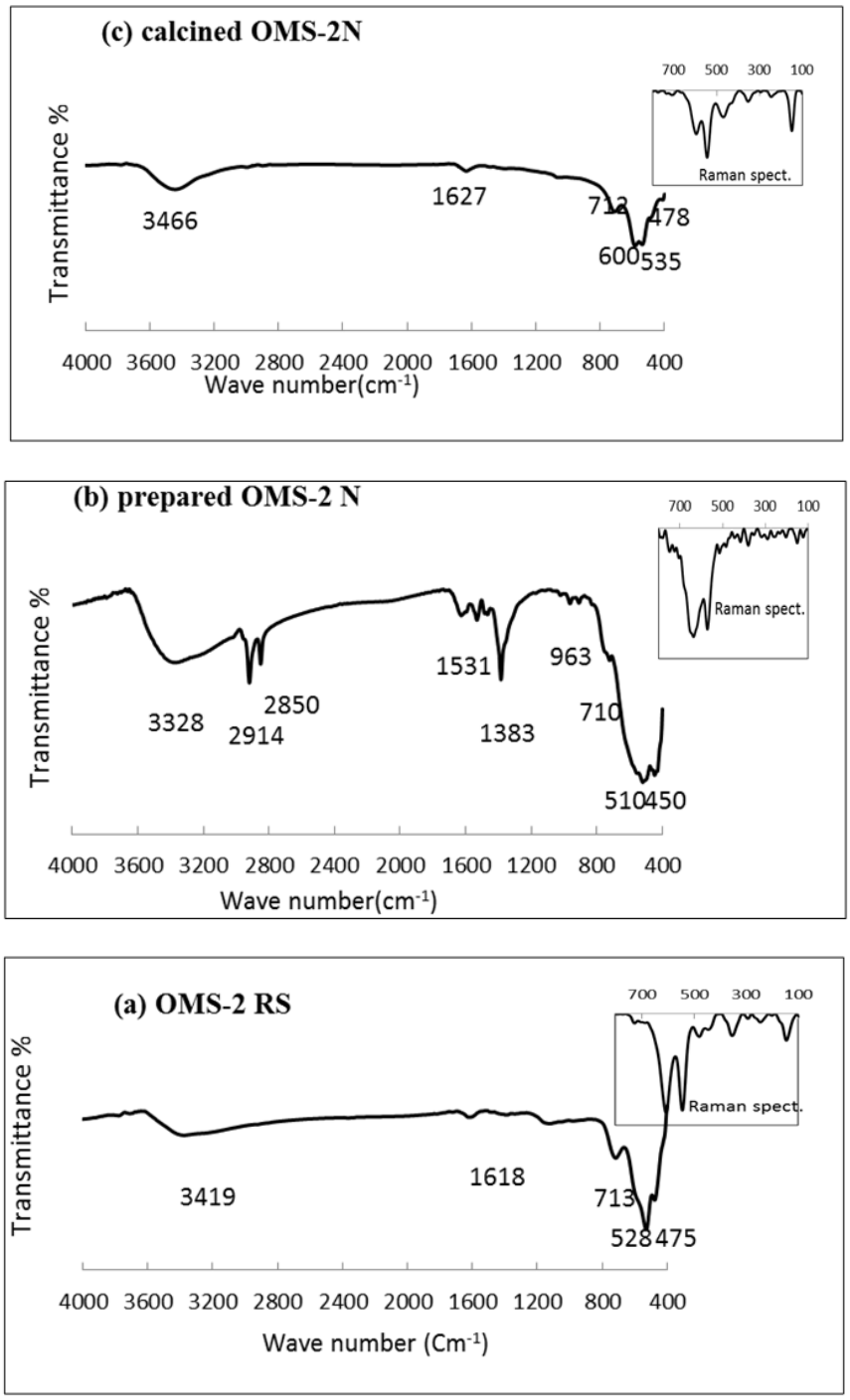

Fig.2. FT-IR and Raman Spect. Of (a) K-OMS-2RS (b) prepared K-OMS-2N& (c) calcined K-OMS-2N samples.

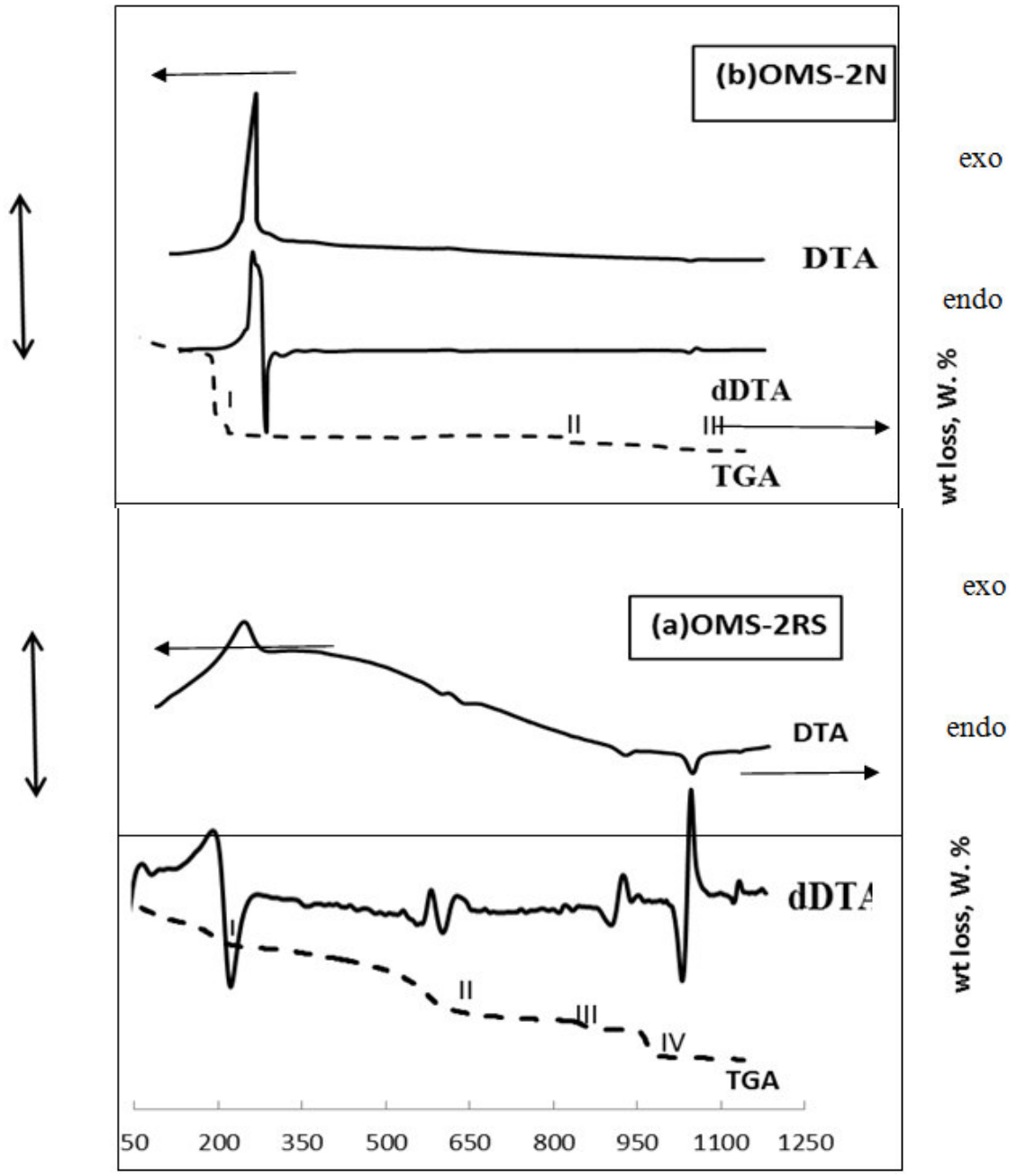

Fig.3. Differential and gravimetric thermal profiles of (a) K-OMS-2RS & (b) K-OMS-2Nsamples.

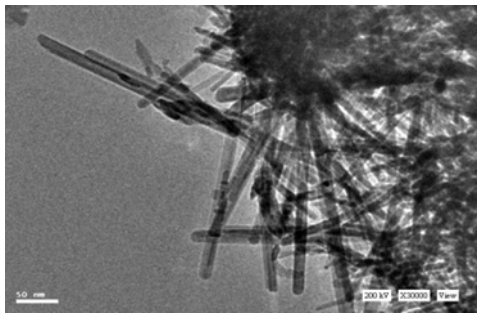

Fig.4. TEM image of K-OMS-2RS sample

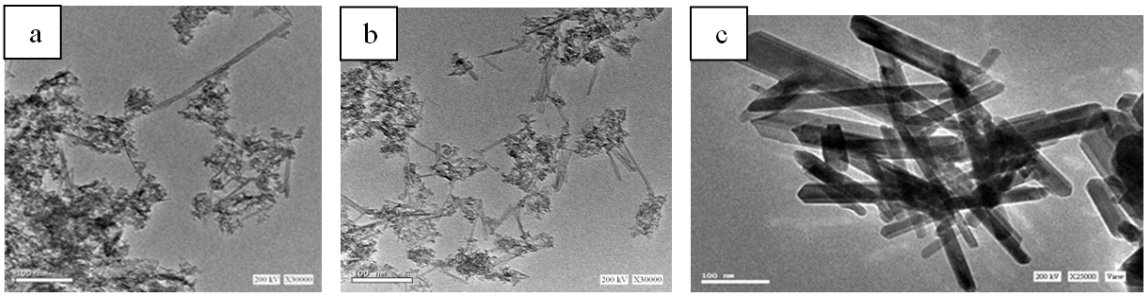

Fig.5. TEM images of K-OMS-2N **(a)un calcined (b) calcined at 200 ^{o}C& (c) calcined at 600 ^{o}C samples.**

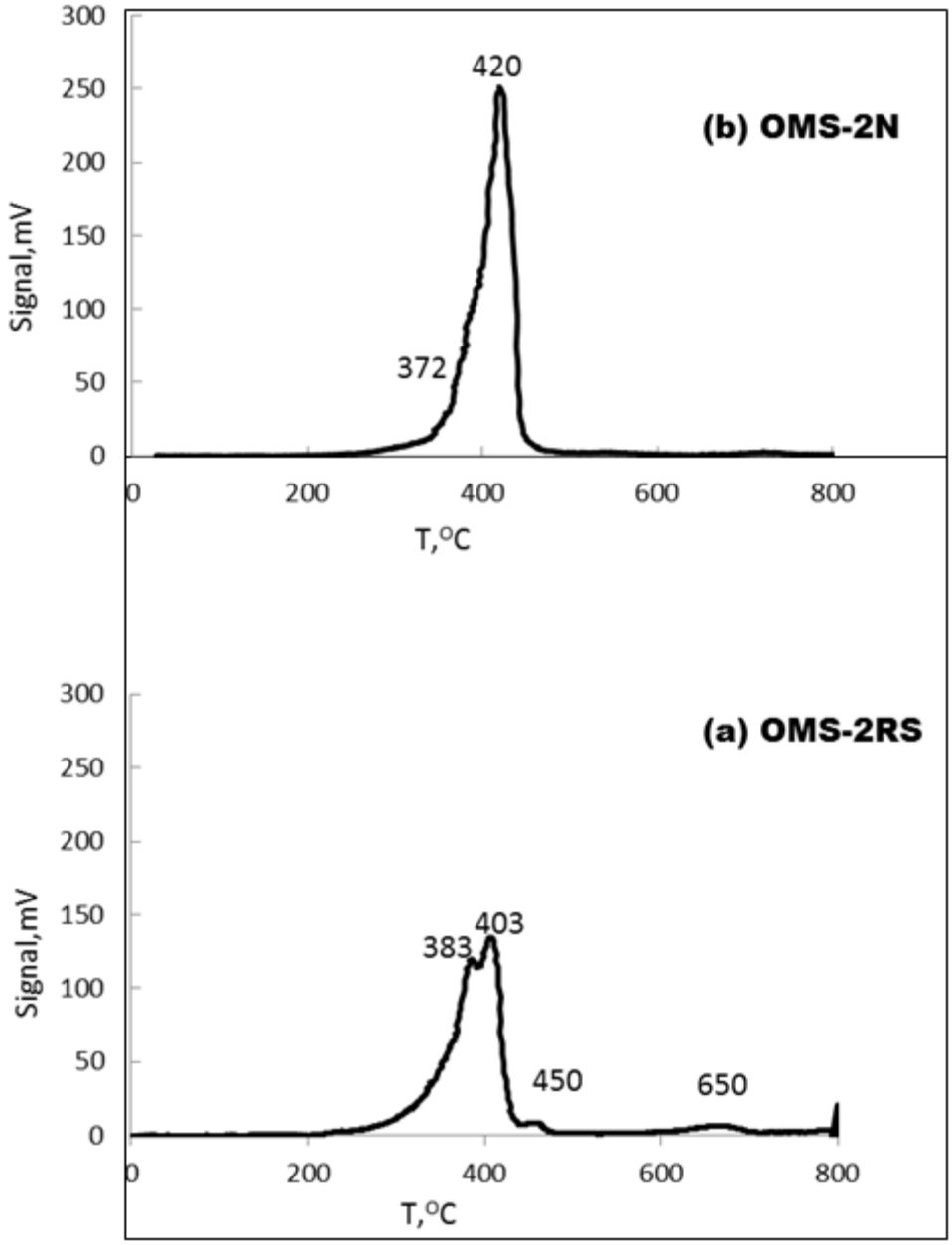

Fig.6. TPR profiles of (a) K-OMS-2RS & (b) K-OMS-2N samples

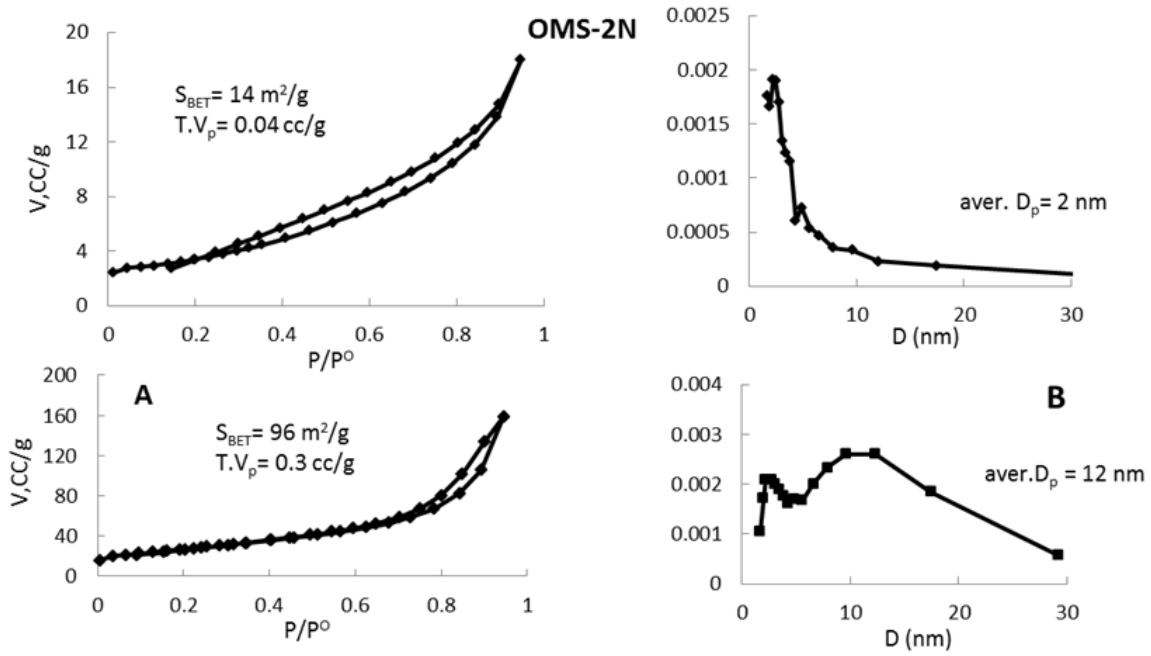

Fig.7. (A) Nitrogen adsorption –desorption isotherms&
(B)Pore size distribution patterns of K-OMS-2RS & K-OMS-2N samples.

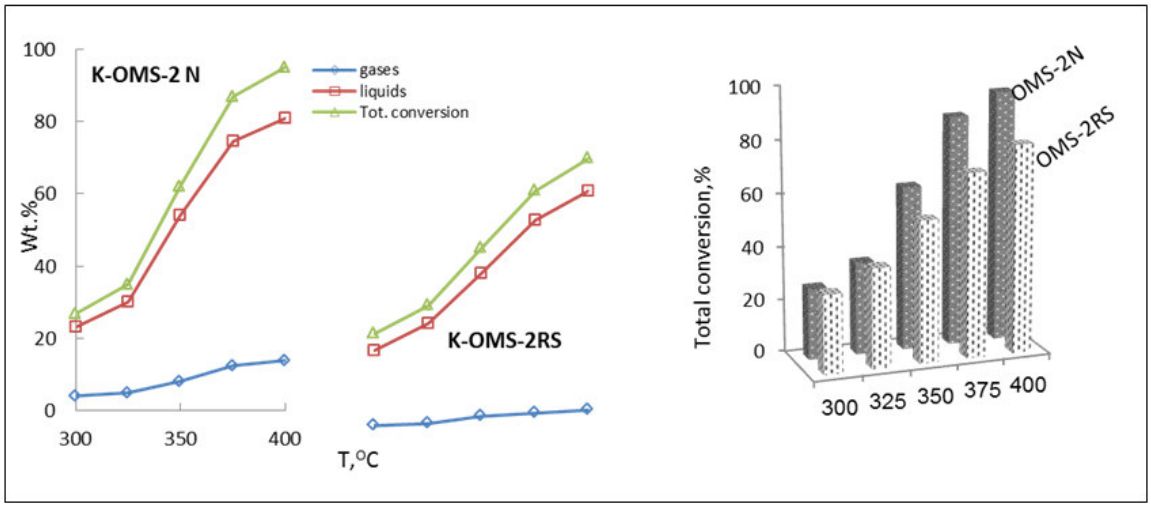

Fig.8. Effect of reaction temperatures on cyclohexane conversion and converted products over K-OMS-RS Samples.

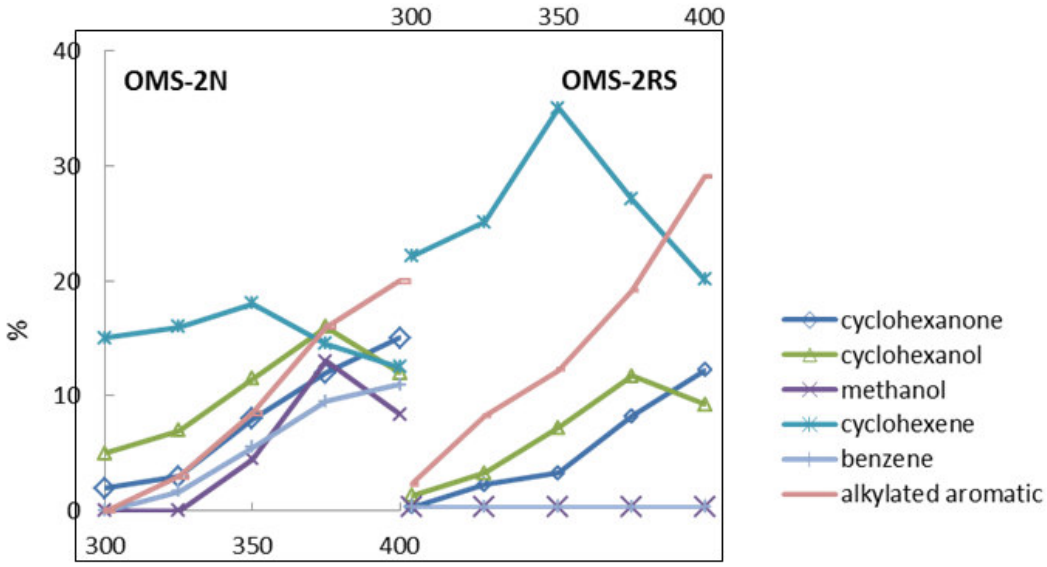

Fig.9. Distribution of the converted products over OMS-2N and OMS-2RS samples at different Reaction temperatures.

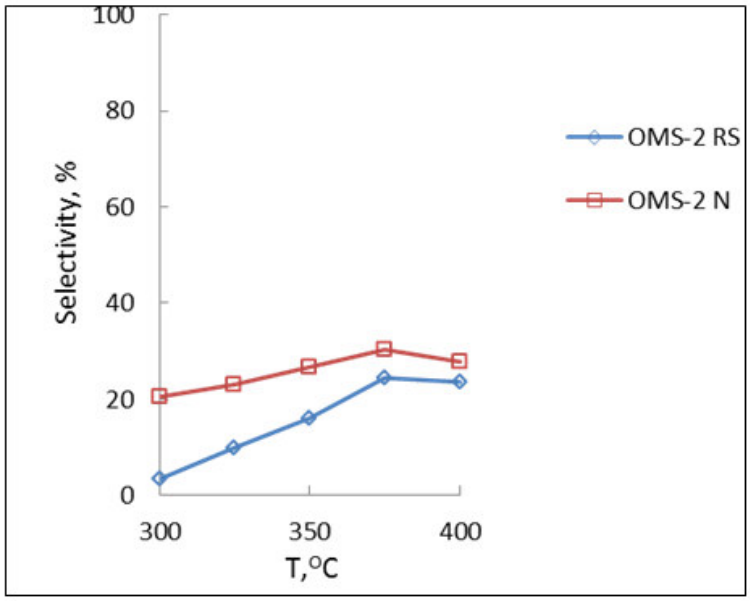

Fig.10. effect of reaction temperatures on selectivity of K-A oil over K-OMS-2N and

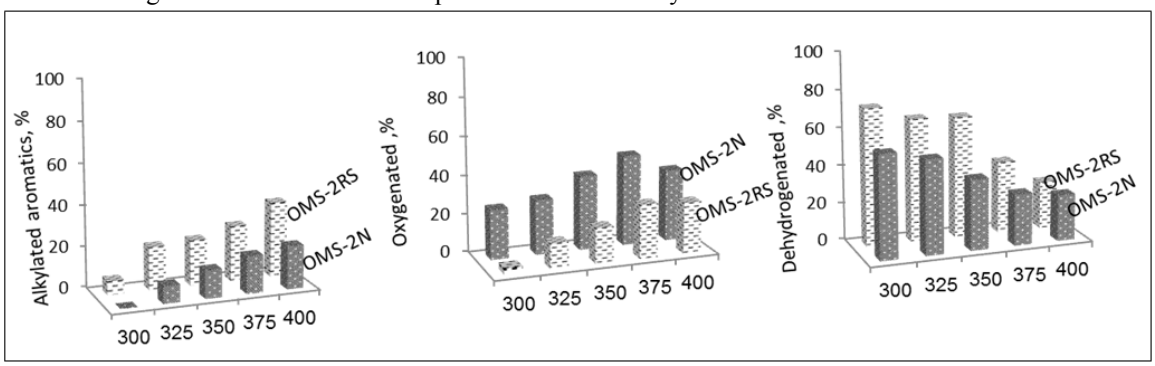

Fig.11. Effect of reaction temperatures on the selectivity of the converted products over OMS-2N and OMS-2RS samples.

The IISTE is a pioneer in the Open-Access hosting service and academic event management. The aim of the firm is Accelerating Global Knowledge Sharing.

More information about the firm can be found on the homepage:
http://www.iiste.org

CALL FOR JOURNAL PAPERS

There are more than 30 peer-reviewed academic journals hosted under the hosting platform.

Prospective authors of journals can find the submission instruction on the following page: http://www.iiste.org/journals/ All the journals articles are available online to the readers all over the world without financial, legal, or technical barriers other than those inseparable from gaining access to the internet itself. Paper version of the journals is also available upon request of readers and authors.

MORE RESOURCES

Book publication information: http://www.iiste.org/book/

Academic conference: http://www.iiste.org/conference/upcoming-conferences-call-for-paper/

IISTE Knowledge Sharing Partners

EBSCO, Index Copernicus, Ulrich's Periodicals Directory, JournalTOCS, PKP Open Archives Harvester, Bielefeld Academic Search Engine, Elektronische Zeitschriftenbibliothek EZB, Open J-Gate, OCLC WorldCat, Universe Digtial Library , NewJour, Google Scholar